BIBECHANA
ISSN 2091-0762 (Print), 2382-5340 (Online)
Journal homepage: http://nepjol.info/index.php/BIBECHANA
Publisher: Department of Physics, Mahendra Morang A.M. Campus, TU, Biratnagar, Nepal

An overview on the non-destructive in-depth surface analysis of corrosion-resistant films: A case study of W-xCr deposits in 12 M HCl solution

Jagadeesh Bhattarai*
Central Department of Chemistry, Tribhuvan University, Kirtipur, Kathmandu, Nepal
*Email: bhattarai_05@yahoo.com
https://orcid.org/0000-0003-0058-079X

Article Information:
Received: June 6, 2020
Accepted: June 28, 2020

Keywords:
Non-destructive
Angle-resolved XPS
In-depth analysis
Corrosion-resistant
W-based sputter deposits

ABSTRACT

Non-destructive in-depth analysis of the surface films formed on the sputter-deposited binary W-xCr (x = 25, 57, 91 at %) alloys in 12 M HCl solution open to air at 30 °C was investigated using an angle-resolved X-ray photoelectron spectroscopic (AR-XPS) technique to understand the synergistic corrosion resistance effects of showing very low corrosion rates, even lower than both alloying metals of the deposits. The average corrosion rates of these three tungsten-based sputter deposits found to be more than five orders of magnitude (between 3.1×10^{-3} and 7.2×10^{-3} mm/y) to that of chromium and also nearly one order of magnitude lower than that of tungsten metals. Such high corrosion resistance of the sputter-deposited W-xCr alloys is due to the formation of homogeneous passive double oxyhydroxide film consisting of W^{ox} and Cr^{4+} cations without any concentration gradient in-depth after immersion in 12 M HCl solution open to air at 30 °C from the study of the non-destructive depth profiling technique of AR-XPS. Consequently, both alloying elements of tungsten and niobium are acted synergistically in enhancing high corrosion resistance properties of the alloys in such aggressive electrolyte.

DOI: https://doi.org/10.3126/bibechana.v18i1.29222

1. Introduction

The method of looking into all components distribution in all depths/layers of a thin surface film is called the in-depth surface analysis. It can estimate the in-depth compositional variation of the thin surface (i.e., nano to micrometers) films formed on the solid substances using both destructive and non-destructive spectroscopic techniques like AR-XPS, Auger electron spectroscopy (AES), ion scattering so on. A comprehensive briefing of both the destructive and non-destructive in-depth compositional analyses of the thin solid surfaces was done since the 1970s by various researchers [1-9]. Among these in-depth analysis techniques, the non-destructive AR-XPS

technique has been widely used as one of the promising in-depth compositional analyses of the thin films to investigate chemical constituents, oxidation states, binding energies and electronic structures of the surface films formed on any solid substrates after a valuable contribution of Siegbahn and his co-researchers in the 1970s [10].

In principle, the in-depth information of such thin film depends on the effective escape depth of the ejected photoelectrons, which increases with an increase in the take-off angle of photoelectrons (TOA) relative to the surface of the sample specimen as explained elsewhere [11-15]. Therefore, the apparent compositions of the thin surface films on the corrosion-resistant alloys should be changed with the TOA in the AR-XPS measurements. In general, the surface sensitivity is varied by changing the TOA and hence the intensity signals of the ejected photoelectrons from the sample species are located in the exterior part of the surface films at a low value of the TOA [13].

For corrosion and materials scientists, the AR-XPS technique becomes one of the very viable in-depth surface characterization tools to study the mechanism of very high corrosion-resistant of metals or/and alloys during the last three decades [16-32]. It allows researchers to check out successfully the constitution of homogeneous or heterogeneous passive surface films formed on the corrosion-resistant metal or/and alloys. It is purposeful for pointing out here that the chemically homogeneous nature of amorphous and nano-crystalline alloys are responsible for their high corrosion resistance owing to the formation of uniform protective passive films that can separate the bulk alloy from aggressive solutions [33]. Such sputter-deposited amorphous or nano-crystalline chromium-, molybdenum- and tungsten-based binary and ternary alloys showed higher corrosion resistance properties than those of alloy-constituting elements in very corrosive media [31, 33] as outlined subsequently.

Despite a very few information about the AR-XPS measurements in the early of the 1990s [34], its applications have been widely accepted for the reason out behind showing synergistic corrosion resistance properties of the sputter-deposited binary and ternary chromium-, molybdenum- and tungsten-based alloys in very aggressive electrolytes since 1995 AD. The sputter-deposited amorphous/nano-crystalline chromium-based binary and ternary alloys with alloying metals of niobium [20, 21], titanium [22], zirconium [23], and simultaneous additions of aluminum and molybdenum [17, 18] showed high corrosion resistance properties, mostly due to the formation of the homogeneous oxyhydroxide constituted passive films formed on the respective alloys surface from electrochemical, and XPS with AR-XPS analyses. Furthermore, sputter deposits of the molybdenum-based binary and ternary alloys with alloying metals of tantalum [26], niobium [35], titanium [36], and simultaneous additions of chromium and nickel [37] showed high corrosion resistance properties, mostly due to the formation of homogeneous surface films formed on these sputter-deposited binary and ternary alloys without distinct heterogeneous distribution of ions.

Since tungsten belongs to the same family as chromium and molybdenum metals in the periodic table, similar behavior of showing high corrosion-resistant properties expects for the sputter-deposited tungsten-based binary and ternary alloys in aggressive environments. A small addition of tungsten in stainless steels enhanced their passivity and pitting corrosion resistance properties of [38, 39]. Very few works on the corrosion of different alloys containing small amounts of tungsten was carried out before 1995 [39-43], probably due to its high melting point and difficult to prepare tungsten-based single phase solid solution alloys with high concentrations of tungsten.

To solve such a problem of the preparation of W-based alloys in a wide composition range was successfully solved using the sputter deposition

technique since 1995 AD. The sputter-deposited binary amorphous or nano-crystalline tungsten alloying with metals; chromium [44-47], titanium [48-45], zirconium [29, 53], molybdenum [54-56], niobium [57-60], and tantalum [61-64], nickel [65-67], and ternary W-Cr-Ni [68-71] and W-Cr-Zr [72-79] alloys were prepared in the wide composition range and they showed higher corrosion resistance than those of alloy-constituting metals in corrosive environments of HCl, NaCl, and NaOH solutions.

From conventional XPS analysis, it was reported that the higher corrosion resistance than alloying components of these tungsten-based alloys is considered due to the formation of spontaneously passivated films which are composed of double oxyhydroxide of W^{ox} and cations of the alloying elements. Among these binary and ternary tungsten-based alloys, the W-Ta alloys showed highest corrosion resistance, and comparatively low corrosion resistance behavior among other binary tungsten-based alloys in very aggressive 12 M HCl solution at 30 °C [19, 31], although the sputter-deposited nano-crystalline W-Cr alloys containing up to 91 at % chromium showed significantly higher corrosion resistance than its alloying tungsten and chromium metals [31, 44, 45]. In particular, the corrosion rate of the W-xCr alloys containing 25-91 at % of chromium shows more than five orders of magnitude lower than the sputter-deposited chromium and even nearly one order of magnitude lower than the corrosion rate of the tungsten deposit in 12 M HCl solution at 30 °C as shown in Fig. 1 [31].

However, the sputter-deposited binary Mo-xCr alloys did not exceed their corrosion rates than alloying molybdenum in 12 M HCl [25] which was noted mostly due to the formation of a heterogeneous passive film formed on the alloy surface from the non-destructive in-depth analysis technique of AR-XPS. In this context, this paper focused to study the in-depth distributions of W^{ox} and Cr^{4+} ions in the passive films formed on the binary W-xCr (x = 25, 57, 91 at %) sputter deposits in 12 M HCl solution at 30 °C, open to air using the non-destructive AR-XPS technique which might be further useful to justify higher corrosion resistance properties of the alloys than those of tungsten and chromium metals.

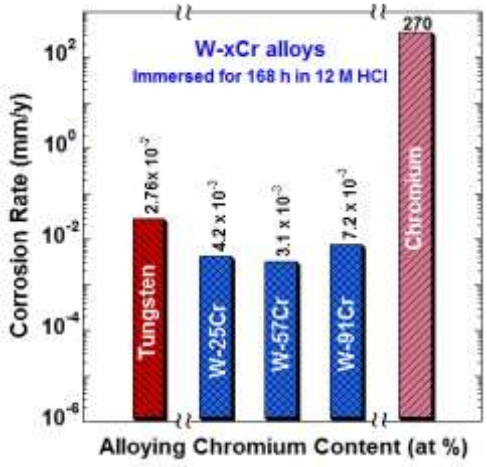

Fig. 1: Corrosion rates of the sputter-deposited tungsten, niobium and W-xNb alloys after immersion for 168 h in 12 M HCl solution open to air at 30 °C [31]

2. Materials and Method

Preparation and characterization of W-xCr alloys

The tungsten alloys containing 25, 57, and 91 atomic percentage (at %) chromium were prepared on glass substrate using DC sputtering machine as described elsewhere [44], and these alloys are called sputter-deposited W-xCr alloys. Three sputter-deposited W-xCr alloys were characterized as nano-crystalline structure having an apparent grain size between 8 and 15 nm [31] from XRD patterns using Scherrer formula as describes elsewhere [54, 80]. Before the immersion tests and AR-XPS analyses, the alloy specimens were mechanically polished with a SiC paper having the grit number 1500 in cyclohexane, degreased by acetone, and dried by blowing dry air to remove the oxide film formed on the surface of the alloys as described elsewhere [81-83]. The average corrosion

rate was estimated using weight loss methods as described elsewhere [84, 85].

In-depth surface analysis of sputter-deposited W-xCr alloys

The in-depth composition of the thin films formed on the W-xCr alloys was analyzed by AR-XPS. Before and after immersion in 12 M HCl solution, XPS spectra were taken using a Shimadzu ESCA–850 photoelectron spectrometer with MgK_α ($h\nu$ = 1253.6 eV) radiation for surface analyses. XPS spectra peaks of tungsten, chromium, carbon, oxygen, and chlorine for the sputter-deposited nano-crystalline W-xCr (x = 25, 57 91 at %) alloys were firstly recorded over a wide binding energy region (that is, 0–1000 eV), and then the most intense peaks of the W 4f, Cr $2p_{3/2}$, C 1s, O 1s, and Cl 2p electrons were recorded in the binding energy range of 20 eV. The peak shift caused by the charging effect was corrected using the C 1s peak, and its value of 285.0 eV was considered for all the measured XRP spectra corrections as recommended elsewhere [86]. For the alloy specimens after immersed in 12 M HCl solution, a very weak Cl 2p spectrum was detected at about 199.0 eV. However, the concentration of the chloride ion was not considered for the quantitative analyses of the surface films in this study because the intensity of the chloride ion is very low for quantitative analyses.

The O 1s spectrum was composed of two peaks; the lower binding energy peak at 530.4 eV was assigned to OM oxygen, and the higher binding energy peak at 532.3 eV was assigned to OH oxygen [87, 88]. The OM oxygen corresponds to O^{2-} ions, and OH oxygen corresponds to OH^- ions and bound water in the surface film. The measured spectrum of W 4f electron was separated into W^{ox} 4f (oxidized W) and W^0 4f (metal W) and the measured spectrum of Cr 2p electron was separated into Cr^{3+} $2p_{3/2}$ (oxidized Cr) and Cr^0 $2p_{3/2}$ (metal Cr) for the sputter-deposited W-xCr alloys. Furthermore, the W^0 4f spectrum has consisted of W^{4+} 4f, W^{5+} 4f, and W^{6+} 4f spectra. The integrated intensities of the W^0 4f, W^{4+} 4f, W^{5+} 4f, W^{6+} 4f, Cr^0 2p, and Cr^{4+} 2p were obtained by the same method as those described elsewhere [31]. The photo-ionization cross-section of the W 4f and Cr $2p_{3/2}$ electrons relative to the O 1s electrons used were 2.97 [40] and 1.71 [88], respectively. The in-depth compositions distribution in both the passive films and underlying alloy surfaces were quantitatively determined using three layers model [30] after the integrated intensities of these spectra of the W-xCr alloys were obtained. The angle between the alloy sample specimen surface and the direction of photoelectron to the detector was changed using tilted-specimen holders at 30°, 45°, 60°, and 90° for AR-XPS analysis as discussed elsewhere.

3. Results and Discussion

The average corrosion rates of the sputter-deposited W and Cr metals in 12 M HCl were estimated about 2.76×10^{-2} mm/y and 2.70×10^{2} mm/y, respectively, while it was estimated nearly five orders of magnitude lower than chromium, and also about one order of magnitude lower than tungsten (i.e., about 3.1-7.2 $\times$ 10^{-3} mm/y) as mentioned above. Consequently, it can be said that simultaneous additions of both W and Cr improve the corrosion resistance properties of the sputter-deposited W-25Cr, W-57Cr, and W-91Cr alloys synergistically. The causes of showing such synergistic corrosion resistance effects of tungsten and chromium of the sputter-deposited W-xCr alloys are further studied here using AR-XPS analysis.

AR-XPS analysis of W-xCr alloys

The experimental results of the AR-XPS measurements are helpful to clarify the mechanism of showing the higher corrosion resistance behavior of the sputter-deposited binary W-xCr alloys than those of alloying elements in 12 M HCl solution. Because the in-depth surface analyses of the spontaneously passivated double oxyhydroxide films formed on the W-xCr alloys using AR- XPS analysis give better understandings of the tungsten

and niobium effects in the corrosion- resistant nature of the alloys. The information about the in-depth compositional distribution of metallic and oxidized species and anions in the passive films of the W-xCr alloys might be insightful to know whether the film is homogeneous or not.

The measured spectra of W 4f electrons into the metallic W^0 4f and oxidized W^{ox} 4f, and of Cr 2p electrons Cr^0 $2p_{3/2}$ and Cr^{3+} $2p_{3/2}$ spectra were separated as shown in Figs. 2 and 3 for the W-25Cr and W-57Cr alloys, respectively, in the given conditions. The W^0 4f spectrum consisted of doublet peaks corresponds to W^0 $4f_{7/2}$ and W^0 $4f_{5/2}$ electrons at lower and higher binding energy. Moreover, the W^{ox} 4f spectrum is also composed of three doublets of the overlapped spectra of three oxidized species of W^{4+} $4f_{7/2}$ and W^{4+} $4f_{5/2}$, W^{5+} $4f_{7/2}$ and W^{5+} $4f_{5/2}$, and W^{6+} $4f_{7/2}$ and W^{6+} $4f_{5/2}$ electrons, as shown in Fig. 2. On the other hand, the Cr^{3+} $2p_{3/2}$ and Cr^0 $2p_{3/2}$ spectra consist of lower and higher binding energy peaks corresponding to oxidized and metallic Cr $2p_{3/2}$ electrons, respectively, as shown in Fig. 3. Besides, the metallic and oxidized species for the W-91Cr alloy were also separated at different TOA of photoelectrons which is not shown here, however, the quantitative analysis is discussed subsequently. The quantitative results of the in-depth distributions of the apparent cationic fractions in the passive film surfaces and the apparent atomic fractions in the underlying alloy surfaces of the W-25Cr, W-57Cr, and W-91Cr alloys as a function of TOA of photoelectrons are shown in Fig. 4.

The W^{ox} ion is noticeably enriched with the deficiency of Cr^{3+} ions in the passive films formed on both W-25Cr and W-57Cr alloys as shown in Figs 4(a) and 4(b) without any concentration gradients of both cations in-depth of the film. Therefore, it can be said that immersion for 5 hours or more in 12 M HCI solution at 30 °C results in the preferential dissolution of chromium from the surface films of the W-xCr alloys containing less than 60 at % chromium, and tungsten becomes the main constituent of the passive film. Similar results of the preferential dissolution of chromium and nickel, titanium, and niobium were reported for the high corrosion-resistant W-xCr-yNi [32], W-xTi [30], and W-xNb [89] alloys, respectively, in aggressive 12 M HCl solution. However, the trend of the in-depth distribution of W^{ox} and Cr^{3+} ions in the passive film formed on the surface of chromium-rich W-91Cr alloy is found to differ.

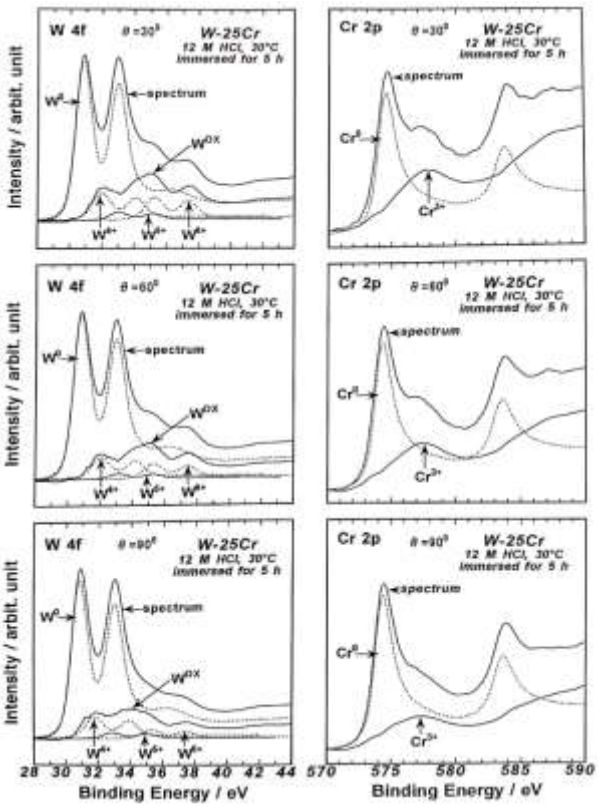

Fig. 2: Examples of the deconvolution of (a) W 4f and (b) Cr 2p spectra measured for the sputter-deposited W-25Cr alloy after 5 h immersion in 12 M HCl solution open to air at 30 °C.

The Cr^{3+} ions are concentrated with a deficiency of W^{ox} ions in the passive film formed on the W-91Cr alloys as shown in Fig. 4(c), although both metal ions are homogeneously distributed in-depth of the passive film. Therefore, it can be said that a significant concentration of tungsten is necessary for maintaining the spontaneous passivation of the sputter-deposited W-25Cr and W-57Cr alloys because chromium is active in 12 M HCl solution [44].

On the other hand, the chromium concentration is slightly higher than tungsten concentration in the passive film formed on the W-91Cr alloys and hence the corrosion resistance properties of the chromium-rich W-91Cr alloy showed nearly two times lower than those of other two tungsten-based alloys containing 25 and 57 at % of chromium as described above in Fig. 1. Furthermore, the metallic W is slightly deficient in the exterior of the underlying alloy surfaces, especially for W-25Cr and W-57Cr alloys, at low TOA but it is found to be almost the same as in alloy composition. Consequently, it can be said that both tungsten and chromium ions are homogeneously distributed in-depth of the thin passive films formed on the sputter-deposited W-xCr alloys after immersion in 12 M HCl solution at 30 °C which should be one of the reasons behind showing of the synergistic corrosion resistance properties by these sputter-deposited binary alloys in very an aggressive environment like 12 M HCl solution.

The similar type of the synergistic effects of the higher corrosion resistance properties of the sputter-deposited binary [21, 23, 27, 28, 30, 31] and ternary [17, 18, 32] alloys than their respective alloying elements were reported in aggressive electrolytes mostly due to the formation of homogeneous passive films formed on the alloys from AR-XPS analysis. It was reported that there was no concentration gradient of tungsten and titanium ions in-depth of the passive surface film and the underlying alloy surface of the sputter-deposited W-xTi alloys after their exposure for 24 hours or more in 12 M HCl solution at 30 °C [30]. Hence, it was presumed that such W-xTi alloys showed significantly high corrosion resistance properties in such an aggressive chloride-containing environment [31]. The enrichment of chromium through its migration and diffusion at the outermost surface of the passive film formed on the sputter-deposited Al-36Cr-9Mo alloy in 1 M HCl solution which was attributed to the faster dissolution of aluminum cations into the solution in comparison with that of chromium cations [17].

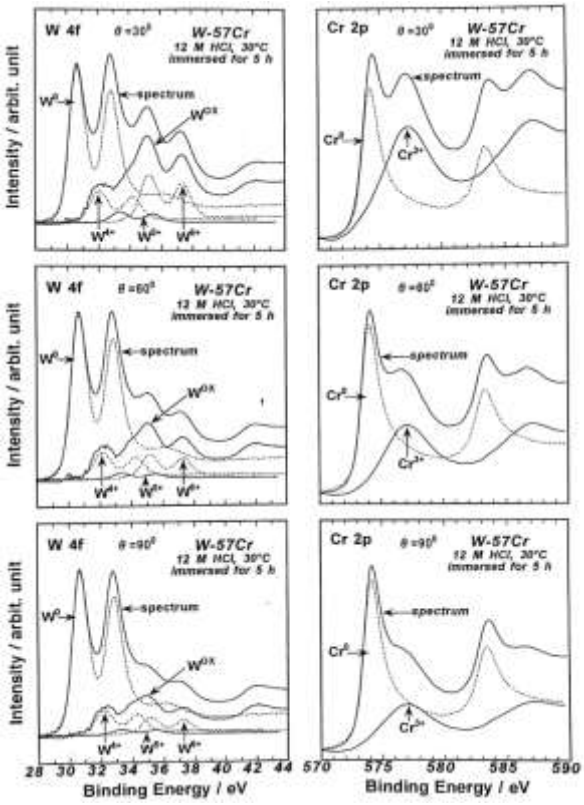

Fig. 3: Examples of the deconvolution of the (a) W 4f and (b) Cr 2p spectra measured for the sputter-deposited W-57Cr alloy after 5 h immersion in 12 M HCl solution open to air at 30 °C.

Moreover, the quantitative analysis of the total W^{ox} ions in different layers/depths of the passive films of the W-xCr alloys were done as a function of TOA of photoelectrons, and the results of the changes of the concentration ratios of W^{4+}, W^{5+}, and W^{6+} ions to the total tungsten ions in the depth of the W-25Cr and w-57Cr alloy surfaces as a function of TOA are shown in Fig. 5. The W^{6+} ion ratio in the passive films formed on both the alloys is significantly higher than those of the ratios of W^{4+} and W^{5+} ions in the exterior parts of the passive films, and the W^{6+} ion decreases with the increasing of TOA, while W^{4+} ion increases with TOA. The ratio of W^{5+} ion remains almost constant with the TOA.

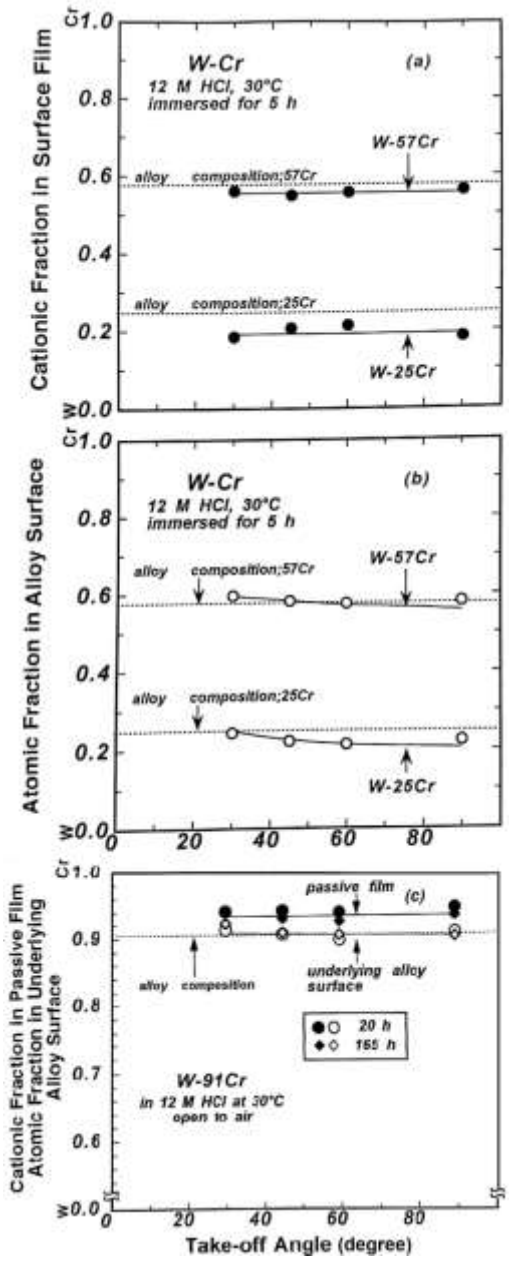

Fig. 4: Changes of the apparent cationic fractions in the passive surface films and atomic fractions in the underlying alloy surfaces of the W-25Cr, 9W-57Cr, and W-91Cr alloys after immersion in 12 M HCl open to air at 30 °C, as a function of TOA of photoelectrons

Accordingly, W^{4+} ion is particularly concentrated in the interior (at 90° TOA) of the passive film formed on the sputter-deposited W-xCr alloys, while the concentration of W^{6+} ion is higher in the exterior (30 to 60° TOA) of the spontaneously passivated films. Accordingly, the relative ratio of W^{6+} ion is higher in the exterior of the surface films and decreases with the depth of the passive film.

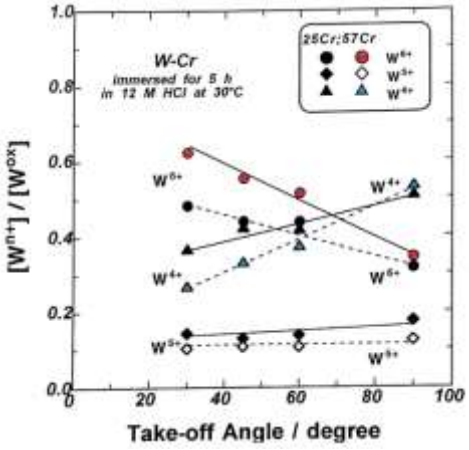

Fig. 5: Concentration ratios of W^{4+}, W^{5+}, and W^{6+} ions to the total tungsten ions (W^{ox}) in the passive films formed on the W-25Cr and W-57Cr alloys.

It is accepted by the corrosionists that the concentration of oxygen species present in the corrosion resistance passive films of the alloys is one of the characteristic properties. Figure 6 shows the qualitative information of the in-depth distribution of oxygen species in which examples of deconvolution of the O 1s spectra measure for the sputter-deposited W-25Cr alloy at 30°, 45°, 60°, and 90° TOA of photoelectrons in the given conditions are shown in Fig. 7. The alloy consists of a major oxygen species of O^{2-} ion, although the peaks correspond to OH^- ion and bound H_2O at low TOA (that is, at 30°/45°) is remarkably higher than that at high TOA (at 60° and 90°) as shown in Fig. 7.

These results assumed that the ratio of $[O^{2-}]$/[cations] is significantly increased with increasing the TOA of photoelectrons and the ratio of $[OH^-]$/[cations] is decreased with decreasing of the take-off angle of photoelectrons in the passive films of the alloys. Consequently, the interior part of the passive films formed on the sputter-deposited W-xCr alloys is rather dry and well developed by M–O–M bridging, while the exterior part of the passive films formed on the alloys is slightly wet with OH^- ion and H_2O. Formation of such type of passive films on the alloy surface might be one of the reasons for showing significantly high corrosion resistance properties by

the sputter-deposited nano-crystalline binary W-xCr alloys than those of their alloy constituting elements in such aggressive 12 M HCl solution. A similar kind of in-depth surface analysis results were reported from the previous studies for the corrosion-resistant sputter-deposited binary and ternary tungsten [27, 28, 30, 32, 89]-, molybdenum [17, 18, 21, 23]-, and chromium [25]- based alloys in very corrosive environments.

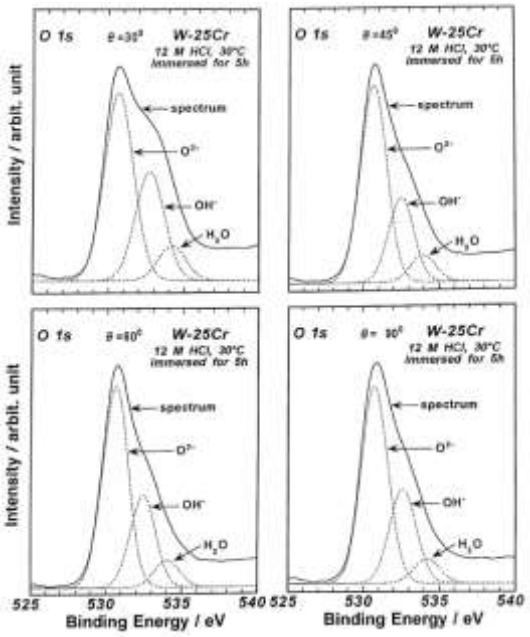

Fig. 6: Examples of the deconvolution of O 1s spectra measured for the sputter-deposited W-26Nb alloy after immersion for 5 h in 12 M HCl at 30 °C at (a) 15°, (b) 30°, (c) 60°, and (d) 90° of TOA (θ)

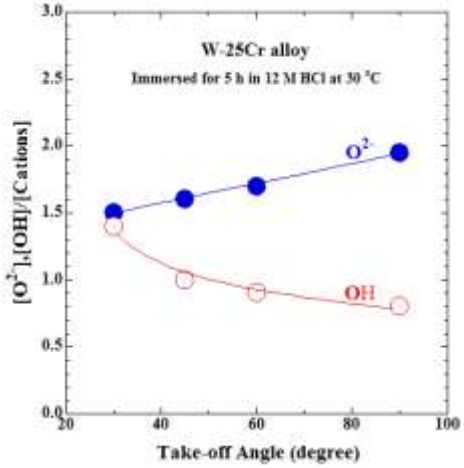

Fig. 7: Ratios of $[O^{2-}]$/[cations] and $[OH^{-}]$/[cations] in the passive films formed on the W-25Cr alloy.

4. Conclusions

This paper was focused to study the in-depth distributions of W^{ox} and Cr^{4+} ions in the passive films formed on the binary W-xCr (x = 25, 57, 91 at %) sputter deposits in 12 M HCl solution at 30 °C, open to air using the non-destructive AR-XPS analysis technique. The synergistic corrosion resistance effects of the simultaneous additions of tungsten and chromium in the sputter-deposited nano-crystalline W-xCr alloys are reasoned out by following findings based on the above discussion.

a) The AR-XPS analyses revealed that all cations of the binary W-xCr alloys are distributed homogeneously in the passivated oxyhydroxide films formed on the alloys.
b) The lower corrosion rates of the W-25Cr, W-57Cr, and W-91Cr alloys than their alloying tungsten and chromium metals are mostly due to the formation of the homogeneous passive films composed of both W^{4+} and Cr^{3+} ions without any concentration gradient in-depth of such oxyhydroxide passive films.
c) The W^{4+} ion is particularly concentrated in the interior of the passivated films formed on all three types of W-xCr alloys, while the concentration of W^{6+} ion is higher in the exterior of the passive films.
d) The interior part of the passive films formed on the W-xCr alloys is rather dry and well developed by M–O–M bridging, while the exterior part of the passive films formed on the alloys is slightly wet with OH^{-} ion and bound H_2O molecule.

Acknowledgments

Author acknowledges to Professors Emeritus; Dr. Koji Hashimoto and Dr. K. Asami of Tohoku University, Sendai, Japan for their kind permission to use the XPS machine, and would like to acknowledge to Profs; Dr. Hiroki Habazaki of Hokkaido University and Dr. Eiji Akiyama of IMR, Tohoku University, Japan for their help and fruitful discussion.

References

[1] A. Harris, Angular dependencies in electron-excited auger emission, Surf. Sci. 15(1) (1969), 77–93. https://doi.org/10.1016/0039-6028(69)90066-1

[2] K. Asami, K. Hashimoto, S. Shimodaira, A trial of non-destructive in-depth surface analysis of Fe–Cr alloys by XPS with different excitation X-ray energies, Trans. Japan Inst. Metals 19(11) (1978) 598–604. https://doi.org/10.2320/matertrans1960.19.598

[3] S. Hofmann, Quantitative depth profiling in surface analysis: A review. Surf. Interface Anal. 2(4) (1980)148−160. https://doi.org/10.1002/sia.740020406

[4] M. Pijolat, G. Hollinger, New depth-profiling method by angular-dependent X-ray photoelectron spectroscopy, Surf. Sci. 105(1) (1981)114−128. https://doi.org/10.1016/0039-6028(81)90151-5

[5] M. N. Rahaman, L. C. De Jonghe, Angle-resolved XPS Analysis of Oxidized Polycrystalline SiC Surfaces, Lawrence Berkeley National Laboratory, University of California, Materials & Molecular Research Division, USA, 1986, P. 20. https://escholarship.org/uc/item/9w7739fq

[6] C. S. Fadley, X-ray photoelectron spectroscopy: Progress and perspectives, J. Electron Spectrosc. Relat. Phenom. 178–179 (2010) 2–32. https://doi.org/10.1016/j.elspec.2010.01.006

[7] S. Tougaard, Energy loss in XPS: Fundamental processes and applications for quantification, non-destructive depth profiling and 3D imaging, J. Electron Spectrosc. Relat. Phenom. 178-179 (2010) 128–153. https://doi.org/10.1016/j.elspec.2009.08.005

[8] S. R. Bare, A. Knop-Gericke, D. Teschner, M. Hävacker, R. Blume, T. Rocha, R. Schlögl, A. S. Y. Chan, N. Blackwell, M. E. Charochak, V. Veen, H. H. Brongersma, Surface analysis of zeolites: An XPS, variable kinetic energy XPS, and low energy ion scattering study, Surf. Sci. 648 (2016) 376–382. https://doi.org/10.1016/j.susc.2015.10.048

[9] I. N. Demchenko, Y. Melikhov, Y. Syryanyy, I. Zaytseva, P. Konstantynoy, M. Chernyshova, Effect of argon sputtering on XPS depth-profiling results of Si/Nb/Si, J. Electron Spectrosc. Relat. Phenom. 224 (2018) 17–22. https://doi.org/10.1016/j.elspec.2017.09.009

[1]. K. Siegbhahn, C. Nordling, A. Fahlman, R. Nordberg, K. Hamrin, J. Hedman, G. Johnssaon, T. Bergmark, S. E. Karlsson, I. Lindgren, B. Lindberg, ESCA-atomic, molecular and solid state studied by means of electron spectroscopy. Uppsala, Sweden: Almquist and Wiksells, 1967.

[11] R.-G. Ciocarlan, I. Arcon, A. Pui, M. Mertens, N. N. Tusar, E. M. Seftel, P. Cool, In-depth structural characterization and magnetic properties of quaternary ferrite systems $Co_{0.5}Zn_{0.25}M_{0.25}Fe_2O_4$ (M = Ni, Cu, Mn, Mg). J. Alloys Comp. 816 (2020) 152674. https://doi.org/10.1016/j.jallcom.2019.152674

[12] R. J. Baird, C. S. Fadley, X-ray photoelectron angular distributions with dispersion-compensating X-ray and electron optics, Journal of Electron Spectroscopy and Related Phenomena 11(1) (1974) 39−65. https://doi.org/10.1016/0368-2048(77)85047-0

[13] C. S. Fadley, Instrumentation for surface studies: XPS angular distributions, J. Electron Spectrosc. Relat. Phenom. 5(1) (1974) 725−754. https://doi.org/10.1016/0368-2048(74)85048-6

[14] S. Tougaard, A. Ignatiev, Concentration depth profiles by XPS; A new approach, Surf. Sci., 129 (2-3) (1983) 355–365. https://doi.org/10.1016/0039-6028(83)90186-3

[15] W. A. Fraser, J. V. Florio, W. N. Delgass, W. D. Robertson, Surface sensitivity and angular dependence of X-ray photoelectron spectra, Surf. Sci. 36(2)(1973)661−674. https://doi.org/10.1016/0039-6028(73)90410-X

[16] K. Asami, S. C. Chen, H. Habazaki, K. Kawashima, K. Hashimoto, A photo-electrochemical and ESCA study of passivity of amorphous nickel-valve metal alloys, Corros. Sci. 31 (1990) 727−732. https://doi.org/10.1016/0010-938X(90)90188-B

[17] E. Akiyama, A. Kawashima, K. Asami, K. Hashimoto, A study of the structure of a passive film using angle-resolved X-ray photoelectron spectroscopy, Corros. Sci. 38(7) (1996) 1127−1140. https://doi.org/10.1016/0010-938X(96)81813-0

[18] E. Akiyama, A. Kawashima, K. Asami, K. Hashimoto, An angle-resolved XPS study of the in-depth structure of passivated amorphous aluminum alloys, Corros. Sci. 39(8) (1997) 1351−1364. https://doi.org/10.1016/S0010-938X(97)00034-6

[19] K. Hashimoto, J. Bhattarai, X. Y. Li, P. Y. Park, E. Akiyama, H. Habazaki, A. Kawashima, K. Asami, Spontaneously passivated sputter-deposited binary alloys with higher corrosion resistance than alloy components. In Proceedings of the Symposium on Passivity and its Breakdown (eds. P. M. Natishan, H. S. Isaacs, M. Janik-Czachor, V. A. Macagno, P. Marcus & M. Seo), Vol. 97-26 (1998), pp. 369−383. Pennington, NJ, USA: The Electrochemical Soc., Inc.

[20] X. Y. Li, E. Akiyama, H. Habazaki, A. Kawashima, K. Asami, K. Hashimoto, An XPS

study of passive films on sputter-deposited Cr-Nb alloys in 12 M HCl solution, Corros. Sci. 40(4-5) (1998), 821−838. https://doi.org/10.1016/S0010-938X(98)00003-1

[21] M. Mehmood, E. Akiyama, H. Habazaki, A. Kawashima, K. Asami, K. Hashimoto, Effects of nanocrystalline heterogeneity on the corrosion behavior of sputter-deposited chromium-niobium alloys, Corros. Sci. 42(2) (2000) 361−382. https://doi.org/10.1016/S0010-938X(99)00077-3

[22] X. Y. Li, E. Akiyama, H. Habazaki, A. Kawashima, K. Asami, K. Hashimoto, Spontaneously passivated films on sputter-deposited Cr-Ti alloys in 6 M HCl solution, Corros. Sci. 39(5) (1997) 935−948. https://doi.org/10.1016/S0010-938X(97)81159-6

[23] X. Y. Li, E. Akiyama, H. Habazaki, A. Kawashima, K. Asami, K. Hashimoto, An XPS study of passive films on corrosion-resistant Cr-Zr alloys prepared by sputter deposition, Corros. Sci. 39(8) (1997) 1365−1380. https://doi.org/10.1016/S0010-938X(97)00035-8

[24] P. Marcus, Surface science approach of corrosion phenomena, Electrochim. Acta 43(1-2) (1998) 109−118. https://doi.org/10.1016/S0013-4686(97)00239-9

[25] P. Y. Park, E. Akiyama, A. Kawashima, K. Asami, K. Hashimoto, The corrosion behavior of sputter-deposited Cr-Mo alloys in 12 M HCl solution, Corros. Sci. 37(11) (1995) 1843−1860. https://doi.org/10.1016/0010-938X(95)00090-7

[26] P. Y. Park, E. Akiyama, A. Kawashima, K. Asami, K. Hashimoto, The corrosion behavior of sputter-deposited Mo-Ta alloys in 12 M HCl solution, Corros. Sci. 38(3) (1996) 397−411. https://doi.org/10.1016/0010-938X(96)00134-5

[27] J. Bhattarai, A non-destructive compositional analysis of thin surface films formed on W-xTa Alloys by angle-resolved X-ray photoelectron spectroscopy, Bibechana 8 (2012) 8−16. https://doi.org/10.3126/bibechana.v8i0.4784

[28] J. Bhattarai, Angle resolver X-ray photoelectron spectroscopic analysis of the passive film of the corrosion-resistant W-32Zr alloy in 12 M HCl solution. Bangladesh J. Sci. Indus. Res. 49(2) (2014)103−110. http://dx.doi.org/10.3329/bjsir.v49i2.22004

[29] J. Bhattarai, E. Akiyama, H. Habazaki, A. Kawashima, K. Asami and K. Hashimoto, Electrochemical and XPS studies of the corrosion behavior of sputter-deposited amorphous W-Zr alloys in 6 and 12 M HCl solutions, Corros. Sci. 39 (1997) 353−375. https://doi.org/10.1016/S0010-938X(97)83351-3

[30] J. Bhattarai, Review on in-depth analysis of the passive films of W-xTi alloys by angle- resolved X-ray photoelectron spectroscopy, Sci. J. Chem. 8(2)(2020)28−35. http://dx.doi.org/10.11648/j.sjc.20200802.12

[31] J. Bhattarai, Tailoring of Corrosion-resistant Tungsten-based Alloys by Sputtering, PhD Thesis, Tohoku University, Sendai, Japan, 1998.

[32] J. Bhattarai, X-ray photoelectron spectroscopic analyses on the corrosion-resistant W-Cr-Ni alloys in 12 M HCl, Trans. Mater. Res. Soc. Japan 35(1) (2010) 1−6. https://doi.org/10.14723/tmrsj.35.1

[33] K. Hashimoto, Chemical properties of rapidly solidified alloys, In H. H. Liebermann (ed.) Rapidly Solidified Alloys; Processes, Structures, Properties, Applications, New York, USA: Marcel Dekker Inc. (1993) pp. 591.

[34] P. J. Cumpson, Angle-resolved XPS and AES: Depth-resolution limits and a general comparison of properties of depth-profile reconstruction methods, J. Electron Spectrosc. Relat. Phenom. 73(1) (1995) 125–152. https://doi.org/10.1016/0368-2048(94)02270-4

[35] P. Y. Park, E. Akiyama, H. Habazaki, A. Kawashima, K. Asami, K. Hashimoto, The corrosion behavior of sputter-deposited Mo-Nb alloys in 12 M HCl solution, Corros. Sci. 38(10) (1996) 1731−1750 https://doi.org/10.1016/S0010-938X(96)00070-4

[36] P. Y. Park, E. Akiyama, H. Habazaki, A. Kawashima, K. Asami, K. Hashimoto, The corrosion behavior of sputter-deposited Mo-Ti alloys in concentrated hydrochloric acids, Corros. Sci. 38(10) (1996) 1649−1667. https://doi.org/10.1016/S0010-938X(96)00041-8

[37] P. Y. Park, E. Akiyama, H. Habazaki, A. Kawashima, K. Asami, K. Hashimoto, The corrosion behavior of sputter-deposited amorphous Cr-Ni-Mo alloys in 12 M HCl, Corros. Sci. 36(8) (1994) 1395−1410. https://doi.org/10.1016/0010-938X(94)90188-0

[38] N. D. Tomashov, G. P. Chernova, O. N. Marcova, Effect of supplementary alloying elements on pitting corrosion susceptibility of 18Cr-14Ni stainless steel, Corrosion 20(5) (1964) 166t−173t. https://doi.org/10.5006/0010-9312-20.5.166t

[39] H. Habazaki, A. Kawashima, K. Asami, K. Hashimoto, The effect of tungsten on the corrosion behavior of amorphous Fe-Cr-W-P-C alloys in 1 M NaCl, J. Electrochem. Soc. 138(1) (1991) 76−81. https://doi.org/10.1149/1.2085581

[40] A. Kawashima, K. Asami, K. Hashimoto, An XPS study of anodic behavior of amorphous nickel-phosphorus alloys containing chromium, molybdenum or tungsten in 1 M HCl, Corros. Sci. 24(9)(1994)807−823. https://doi.org/10.1016/0010-938X(84)90029-5

[41] G. S. Frankel, R. C. Newman, C. V. Jahnes, M. A. Russak, On the pitting resistance of sputter-deposited aluminum alloys, J. Electrochem. Soc. 140(8) (1993) 2192−2197. https://doi.org/10.1149/1.2220794

[42] Y. Yoshioka, H. Habazaki, A. Kawashima, K. Asami, K. Hashimoto, An XPS study of the corrosion behavior of sputter-deposited amorphous Al-W alloys in 1 M HCl, Corros. Sci. 32(3) (1991), 313−325. https://doi.org/10.1016/0010-938X(91)90076-2

[43] B. A. Shaw, T. L. Fritz, G. D. Davis, W. C. Moshier, The influence of tungsten on the pitting of aluminum films, J. Electrochem. Soc. 137(4) (1990) 1317−1318. https://doi.org/10.1149/1.2086658

[44] J. Bhattarai, E. Akiyama, H. Habazaki, A. Kawashima, K. Asami, K. Hashimoto, Electrochemical and XPS studies on the passivation behavior of sputter-deposited W-Cr alloys in 12 M HCl solution, Corros. Sci. 40(2-3) (1998), 155−175. https://doi.org/10.1016/S0010-938X(97)00106-6

[45] J. Bhattarai, The role of tungsten in the passivation behavior of sputter-deposited Cr-9W alloy in 12 M HCl, J. Inst. Sci. Technol., 12 (2002), 125−138.

[46] M. Basnet, J. Bhattarai, The corrosion behavior of sputter-deposited nano-crystalline W-Cr alloys in NaCl and NaOH solution, J. Nepal Chem. Soc. 25 (2010)53−61. https://doi.org/10.3126/jncs.v25i0.3300

[47] J. Bhattarai, K. Hashimoto, X-ray photoelectron spectroscopy study in the anodic passivity of sputter-deposited nano-crystalline W-Cr alloys in 12 M HCl, Tribhuvan Univ. J. 21(2) (1998) 1−16. https://doi.org/10.3126/tuj.v21i2.4568

[48] J. Bhattarai, E. Akiyama, A. Kawashima, K. Asami, K. Hashimoto, The corrosion behavior of sputter-deposited amorphous W-Ti alloys in 6 M HCl solution, Corros. Sci. 37(12) (1995) 2071−2086. https://doi.org/10.1016/0010-938X(95)00120-9

[49] J. Bhattarai, K. Hashimoto, The anodic passivity of sputter-deposited W-Ti alloys in hydrochloric solutions, Nepal J. Sci. Technol. 4(1) (2002) 37−43. http://www.nast.org.np/njst/index.php/njst/article/view/84/69

[50] J. Bhattarai, The corrosion behavior of sputter-deposited W-Ti alloys in 0.5 M NaCl solution, Nepal J. Sci. Technol. 10 (2009) 109−114. http://dx.doi.org/10.3126/njst.v10i0.2899

[51] A. Sharmah, H. Jha, J. Bhattarai, The passivation behavior of sputter-deposited W-Ti alloys in 1 M NaOH solution, J. Nepal Chem. Soc. 22 (2007) 17−25. https://doi.org/10.3126/jncs.v22i0.518

[52] J. Bhattarai, The confocal scanning laser microscopic study of the pitting corrosion on sputter-deposited W-Ti alloys in 1 M NaOH solution, Tribhuvan Univ. J. 26(1) (2009) 17−26. https://doi.org/10.3126/tuj.v26i1.2611

[53] P. Shrestha and J. Bhattarai, The passivation behavior of sputter-deposited W-Zr alloys in NaCl and NaOH solutions, J. Nepal Chem. Soc. 25 (2010) 37−45. http://dx.doi.org/10.3126/jncs.v25i0.3283

[54] J. Bhattarai, Structure and corrosion behavior of sputter-deposited W-Mo alloys, J. Nepal Chem. Soc.21(2006)19−25. https://doi.org/10.3126/jncs.v21i0.217

[55] J. Bhattarai, The passivation behavior of sputter-deposited W-xMo alloys in 0.5 M NaCl solution, Sci. World 10 (2012) 29−32. https://doi.org/10.3126/sw.v10i10.6858

[56] A. Khadka, J. Bhattarai, Corrosion and electrochemical properties of nano-crystalline W-Mo alloys in NaOH solution, Nepal J. Sci. Technol. 11(2014)147−151. https://doi.org/10.3126/njst.v11i0.4137

[57] J. Bhattarai, E. Akiyama, H. Habazaki, A. Kawashima, K. Asami, K. Hashimoto, Electrochemical and XPS studies of the corrosion behavior of sputter-deposited W-Nb alloys in concentrated hydrochloric acid solutions, Corros. Sci. 40(1) (1998) 19−42. https://doi.org/10.1016/S0010-938X(97)00108-X

[58] J. Bhattarai, E. Akiyama, H. Habazaki, A. Kawashima, K. Asami, K. Hashimoto, The influence of concentration of hydrochloric acid solutions on the passivation behavior of sputter-deposited tungsten rich W-Nb alloys, Corros. Sci. 40(11) (1998) 1897−1914. https://doi.org/10.1016/S0010-938X(98)00088-2

[59] H. Jha, J. Bhattarai, Corrosion behavior of sputter-deposited W-Nb alloys in NaCl and NaOH solutions, J. Alloys Comp. 456 (2008) 474−478. https://dx.doi.org/10.1016/j.jallcom.2007.02.100

[60] J. Bhattarai, X-ray photoelectron spectroscopic study on the anodic passivity of sputter-deposited W-Nb alloys in 12 M HCl solution, J. Sci. Res. 3(3) (2011) 467−480. https://dx.doi.org/10.3329/jsr.v3i3.7207

[61] J. Bhattarai, E. Akiyama, H. Habazaki, A. Kawashima, K. Asami, K. Hashimoto, The passivation behavior of sputter-deposited W-Ta alloys in 12 M HCl, Corros. Sci. 40(4-5) (1998) 757−779. https://doi.org/10.1016/S0010-938X(97)00177-7

[62] J. Bhattarai, X-ray photoelectron spectroscopic study on the anodic passivity of sputter-deposited W-Ta alloys in 12 M HCl, Nepal J. Sci. Technol.

12(2011)139−148.
https://doi.org/10.3126/njst.v12i0.6492

[63] J. Bhattarai, S. Baral, The corrosion behavior of sputter-deposited W-xTa alloys in 0.5 M NaCl solution, Nepal J. Sci. Technol. 14(1) (2013) 103−108.
https://doi.org/10.3126/njst.v14i1.8929

[64] S. Baral, J. Bhattarai, The effect of tantalum addition on the corrosion behavior of W-xTa alloys in 1 M NaOH solution, Bibechana 10 (2014) 1−8. https://dx.doi.org/10.3126/bibechana.v10i0.8363

[65] J. Bhattarai, Electrochemical and XPS studies on the corrosion behavior of sputter-deposited amorphous W-Ni alloys in 12 M HCl, J. Nepal Chem. Soc. 20 (2001) 24−40.

[66] S. P. Sah, J. Bhattarai, The electrochemical and surface studies of the corrosion behavior of sputter-deposited W-Ni alloys in 0.5 M NaCl solution, J. Nepal Chem. Soc. 23 (2009) 45−53. https://dx.doi.org/10.3126/jncs.v23i0.2096

[67] J. Bhattarai, S. P. Sah, H. Jha, Electrochemical and surface studies on the passivation behavior of sputter-deposited W-Ni alloys in NaOH solutions, J. Nepal Chem. Soc. 22 (2007) 7−16. https://doi.org/10.3126/jncs.v22i0.517

[68] J. Bhattarai, The effects of chromium and nickel on the passivation behavior of sputter-deposited W-Cr-Ni alloys in 12 M HCl solution, Sci. World 7(7) (2009)24−28.
https://doi.org/10.3126/sw.v7i7.3819

[69] P. L. Kharel, S. P. Sah, J. Bhattarai, Roles of alloying elements on the passivity of W-xCr-yNi alloys in aggressive environments, Nepal J. Sci. Technol.14(2)(2013)73−80.
http://dx.doi.org/10.3126/njst.v14i2.10418

[70] J. Bhattarai, P. L. Kharel, Effects of chromium and tungsten on the corrosion behavior of sputter-deposited W-Cr-Ni alloys in 0.5 M NaCl solution, J. Inst. Sci. Technol. 16 (2009) 141−151.

[71] P. L. Kharel, J. Bhattarai, The corrosion behavior of sputter-deposited W-Cr-(4-15)Ni alloys in NaOH solution, J. Nepal Chem. Soc. 24 (2009) 3−11.
http://dx.doi.org/10.3126/jncs.v24i0.2380

[72] J. Bhattarai, The corrosion behavior of sputter-deposited ternary Zr-(12-18)Cr-W alloys in 12 M HCl solution, J. Nepal Chem. Soc. 26 (2010) 13−21.
https://doi.org/10.3126/jncs.v26i0.3625

[73] J. Bhattarai, The corrosion behavior of sputter-deposited ternary W-Zr-(15-18)Cr alloys in 12 M HCl, Afr. J. Pure Appl. Chem. 5(8) (2011) 212−218.

[74] J. Bhattarai, Role of alloying elements on the corrosion behavior of sputter-deposited amorphous W-Cr-Zr alloys in 0.5 M NaCl solution, Sci. World 9(2011)34−38.
http://dx.doi.org/10.3126/sw.v9i9.5515

[75] B. R. Aryal, J. Bhattarai, Effects of tungsten, chromium and zirconium on the corrosion behavior of ternary amorphous W-Cr-Zr alloys in 1 M NaOH solution, Sci. World 9 (2011) 39−43. http://dx.doi.org/10.3126/sw.v9i9.5516

[76] J. Bhattarai, Effects of tungsten, zirconium and chromium on the passivity of sputter-deposited W-Zr-Cr alloys in aggressive environments, In 18th International Corrosion Congress 20-24 November, 2011 (pp. 4), Perth, WA, Australia. https://www.researchgate.net/publication/341267131

[77] R. R. Kumal, J. Bhattarai, Roles of alloying elements on the corrosion behavior of amorphous W-Zr-(15-33)Cr alloys in 1 M NaOH solution, J. Nepal Chem. Soc. 25 (2010) 93−100. http://dx.doi.org/10.3126/jncs.v25i0.3312

[78] B. R. Aryal, J. Bhattarai, Effects of alloying elements on the corrosion behavior of sputter-deposited Zr-(12-21)Cr-W alloys in 0.5 M NaCl solution, J. Nepal Chem. Soc. 25 (2010) 75−82. https://dx.doi.org/10.3126/jncs.v25i0.3305

[79] D. B. Subedi, D. B. Pokharel, J. Bhattarai, Study the corrosion inhibition mechanism of sputter-deposited W-42Cr-5Ni and Cr-10Zr-10W alloys by sodium nitrite as green inhibitor in 0.5 M NaCl and 1 M NaOH solutions, Intl. J. Appl. Sci. Biotechnol. 2(4)(2014)537−543.
http://dx.doi.org/10.3126/ijasbt.v2i4.11531

[80] B. D. Cullity, Diffraction I: The directions of diffracted beams, In Elements of X-ray Diffraction (1st edition), Chapter-3, Addison-Wesley Publ. Co. Inc. (1956). pp.98−100. https://archive.org/details/elementsofxraydi030864mbp/page/n13/mode/2up

[81] B. N. Subedi, K. Amgain, S. Joshi, J. Bhattarai, Green approach to corrosion inhibition effect of Vitex negundo leaf extract on aluminum and copper metals in biodiesel and its blend, Int. J. Corros. Scale Inhib. 8(3) (2019) 744−759. https://doi.org/10.17675/2305-6894-2019-8-3-21

[82] M. Rana, S. Joshi, J. Bhattarai, Extract of different plants of Nepalese origin as green corrosion inhibitor for mild steel in 0.5 M NaCl solution, Asian J. Chem. 29(5) (2017) 1130−1134. https://doi.org/10.14233/ajchem.2017.20449

[83] D. B. Pokharel, D. B. Subedi, J. Bhattarai, Study the effect of sodium nitrite as a green inhibitor for the sputter-deposited tungsten-based ternary alloys in 0.5 M NaCl solution, Bibechana 12 (2015) 1−12. http://dx.doi.org/10.3126/bibechana.v12i0.11670

[84] J. Bhattarai, D. B. Pokharel, D. B. Subedi, D. VK, Effects of tungsten and nitrite ions as corrosion

inhibitor for Cr-10Zr-10W alloy in 0.5 M NaCl solution, Int. J. Metall. Alloys 5(1) (2019) 11−19.

[85] J. Bhattarai, M. Rana, M. R. Bhattarai, S. Joshi, Effect of green corrosion inhibitor of Nepalese origin plants for corrosion control of mild steel in aggressive environments, In Proc. CORCON 2018, Sept 30−Oct 3, 2018 (12pp), Jaipur, India: NECE International, Gateway of India Section (NIGIS).

[86] G. Greczynski, L. Hultman, X-ray photoelectron spectroscopy: Towards reliable binding energy referencing, Prog. Mater. Sci., 107 (2020) 100591 (47pp). https://doi.org/10.1016/j.pmatsci.2019.100591

[87] J. Bhattarai, Effects of antimony and tungsten additions in Mn-Mo-Sn oxide electro-catalyst for hydrogen production from electrolysis of 0.5 M NaCl solution, Bangladesh J. Sci. Ind. Res. 47(2) (2012)231−238. https://doi.org/10.3329/bjsir.v47i2.11459

[88] K. Asami, K. Hashimoto, The X-ray photoelectron spectra of several oxides of iron and chromium, Corros. Sci. 17(7) (1977) 559−570. https://doi.org/10.1016/S0010-938X(77)80002-4

[89] J. Bhattarai, An overview on the synergistic corrosion resistance property of tungsten alloys by angle-resolved X-ray photoelectron spectroscopy: A case study of sputter-deposited W-xNb alloys, Ceylon J. Sci., submitted (2020).